

Effective Diversity in Population-Based Reinforcement Learning

Jack Parker-Holder*
University of Oxford
jackph@robots.ox.ac.uk

Aldo Pacchiano*
UC Berkeley
pacchiano@berkeley.edu

Krzysztof Choromanski
Google Brain Robotics
kchoro@google.com

Stephen Roberts
University of Oxford
sjrob@robots.ox.ac.uk

Abstract

Maintaining a population of solutions has been shown to increase exploration in reinforcement learning, typically attributed to the greater diversity of behaviors considered. One such class of methods, *novelty search*, considers further boosting diversity across agents via a multi-objective optimization formulation. Despite the intuitive appeal, these mechanisms have several shortcomings. First, they make use of mean field updates, which induce cycling behaviors. Second, they often rely on handcrafted behavior characterizations, which require domain knowledge. Furthermore, boosting diversity often has a detrimental impact on optimizing already fruitful behaviors for rewards. Setting the relative importance of novelty-versus reward-factor is usually hardcoded or requires tedious tuning/annealing. In this paper, we introduce a novel measure of population-wide diversity, leveraging ideas from Determinantal Point Processes. We combine this in a principled fashion with the reward function to adapt to the degree of diversity during training, borrowing ideas from online learning. Combined with task-agnostic behavioral embeddings, we show this approach outperforms previous methods for multi-objective optimization, as well as vanilla algorithms solely optimizing for rewards.

1 Introduction

Reinforcement Learning (RL) considers the problem of an agent taking actions in a given environment in order to maximize total (discounted/expected) reward [52]. In model-free on-policy RL, an agent seeks to explore the environment in order to generate experience that will help it to learn policies leading to high rewards.

In the *deep* RL paradigm, policies π_θ are typically represented by neural networks, encoded by parameter vectors $\theta \in \mathbb{R}^d$ (their flattened representations) and can be thought of as mappings from states s to actions a (or distributions over actions if the policy is not deterministic).

Neuroevolution methods [49], seek to maximize the reward of a policy through approaches strongly motivated by natural biological processes. Typically a policy, or population of policy parameter vectors (“genotypes”) are perturbed (“mutated”) and their reward (“fitness”) is evaluated in the environment. In the next iteration (“generation”), the individual or population is selected based on their fitness. The simplicity and scalability of these methods have led to their increased popularity in solving RL tasks [42, 3, 2, 4, 51].

*Equal contribution.

This success has led to heightened cross-pollination between the two communities, with population-based methods proving to be an exciting area of research [26, 16, 27]. Similarly to the case of other parallel optimization methods [37], training populations of agents provides the potential benefit of increased exploration of the solution space with the same (wall-clock) training time. In that vein, Quality Diversity (QD, [36]) algorithms are a particularly promising category of neuroevolution methods. QD algorithms explicitly seek high performing policies with diverse behaviors and have been shown to produce striking results, such as increased exploration [4] or adaptive behavior on real hardware [5]. However, they have a few key shortcomings.

The first major problem is cycling. Typically, each agent is updated by taking a gradient step with respect to only its individual contribution to the population’s joint reward-diversity score function. This approach simplifies the many body problem of optimizing a population via a mean field update, and consequently increases the propensity of cycles to arise, whereby different members of the population constantly switch between behaviors. This has the unfortunate effect of preventing any single agent exploiting a promising behavior. This phenomenon motivates the MAP-Elites algorithm [30, 5], whereby only one solution may lie in each quadrant of a pre-defined space, however this relies on human hand engineering of the axis for the grid.

Another well-known flaw of QD algorithms [19] is the use of behavioral characterizations (BCs), which are typically chosen using domain knowledge. For example, in locomotion problems it is common to use the final (x, y) coordinates. While intuitively appealing, the requirement for human expertise limits broader application of these approaches. Interestingly, there have recently been a series of works in the RL community inspired by these methods [14, 6], which do not suffer from this issue. Instead of solely relying on a user defined BC, the behavioral embedding in these methods is simply the actions used by a given agent on an appropriately selected subset of states. Similarity between policies can be measured in the space provided by this behavioral embedding. Incidentally, the geometry induced by these embeddings has already been successfully used in popular trust region algorithms [46, 45].

Finally, promoting diverse behaviors may not always be desirable. Consider the case where there is an accurate and reliable reward function. Diluting it with a multi-objective update may lead to the failure to refine high performing behaviors (e.g. the Humanoid task in [4]). In addition, it has been shown that random initialization may be sufficient to ensure diversity, rendering an explicit objective obsolete [32].

In this paper, rather than focusing on a hand-picked BCs, we define *behavioral embeddings* as the actions taken by a policy on a possibly random set of states (we explore various ways of selecting them in the experimental section, but as we show, uniform sampling works well in practice). More formally let $\{s_1, \dots, s_n\}$ be n states chosen from the set of states visited in the most recent iteration. We define the behavioral embedding corresponding to a policy parameterized by θ as $\Phi(\theta)$ to be the concatenation of actions $a_i = \pi_\theta(a_i | s_i)$ for states $s_i \in \{s_1, \dots, s_n\}$. These embeddings allow us to compare policies’ behavior in regions of the state space not accessible to one of them, while also mitigating the effect of the transition dynamics.

Equipped with these behavioral embeddings, we introduce a new algorithm, *Diversity via Determinants* (DvD), where all members of the population are *jointly* optimized for diversity and rewards. We do this by treating the diversity of the whole population as a blackbox optimization problem and accurately measure it by leveraging insights from Determinantal Point Processes (DPPs, [21]), using determinants of kernel/similarity matrices of behavioral embeddings. In our approach agents are still optimizing for their *local* rewards and this signal is a part of their hybrid objective that also takes into account the *global* goal of the population - its diversity.

Finally, to ensure diversity is promoted *effectively*, we introduce an adaptive mechanism based on Thompson Sampling [39, 40]. This provides us with a principled means to trade-off reward vs. diversity through the lens of multi-armed bandits [47].

We demonstrate in a series of experiments that DvD is able to find diverse, high quality solutions while often finding an optimal policy for a hard exploration environment. Crucially, DvD still performs as well as a single objective approach for simpler tasks, showing the effectiveness of the adaptive mechanism.

This paper is organized as follows. (1) We begin by providing strong motivation for our algorithm in Section 2. (2) In Section 3 we discuss related work in more detail. (3) In Section 4 we explain basic

techniques for optimization via diverse populations. **(4)** In Section 5 we present our DvD algorithm. **(5)** In Section 6 we provide empirical evidence of the effectiveness of DvD. We conclude in Section 7 and provide additional technical details in the Appendix.

2 Motivating Diversity via Determinants

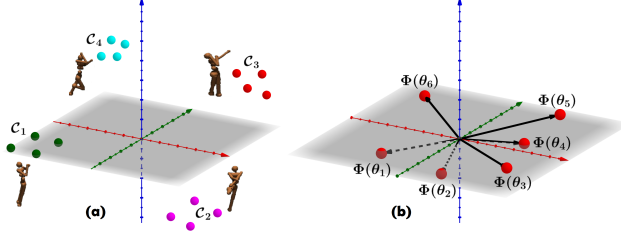


Figure 1: Illustration of problems with standard novelty search exploration. (a): populations of agents split into four clusters with agents within cluster discovering similar policies. (b): embedded policies $\Phi(\theta_1), \dots, \Phi(\theta_6)$ lay in a grey hyperplane. In (a) resources within a cluster are wasted since agents discover very similar policies. In (b) all six embeddings can be described as linear combinations of embeddings of fewer canonical policies. In both settings standard novelty techniques assign high novelty scores but diversity as measured by determinants is low.

Choosing determinants to quantify diversity is crucial. First of all, they prevent the undesirable clustering phenomenon, where a population evolves to a collection of conjugate classes, that standard distance-based methods are not resilient to. To illustrate this point, consider a simple scenario, where all M agents are partitioned into k clusters of size $\frac{M}{k}$ each for $k = o(M)$. By increasing the distance between the clusters one can easily make the novelty measured as an average distance between agents’ embedded policies as large as desired, but that is not true for the corresponding determinants which will be zero if the similarity matrix is low rank. Furthermore, even if all pairwise distances are large, the determinants can be still close to zero if spaces where agents’ high-dimensional policy embeddings live can be accurately approximated by much lower dimensional ones. Standard methods are too crude to measure novelty in such a way (see: Fig. 1).

From a geometric perspective, the determinant of the kernel matrix represents the volume of a parallelepiped spanned by feature maps corresponding to the kernel choice. We seek to maximize this volume, effectively “filling” the feature (or behavior) space.

Another interpretation as to why this may be effective is the ability for DvD to reason one step ahead. Typical novelty search methods assume the remaining members of the population are static. When these agents subsequently move in the behavior space they can induce cycling since the agents are constantly trying to repel from one another. For DvD, each agent has the joint objective of maximizing the population diversity, and thus can consider the changing behavior of all agents simultaneously.

Finally, we show in the Appendix (see: Section 10) for the case of the squared exponential kernel, the first order approximation to the determinant is approximately equal to the mean pairwise L_2 distance. However, for greater population sizes, this first order approximation is zero, implying the determinant comes from higher order terms. We are excited by the potential future work to fully explore these links.

3 Background and Related Work

A Markov Decision Process (MDP) is a tuple $(\mathcal{S}, \mathcal{A}, P, R)$. Here \mathcal{S} and \mathcal{A} stand for the sets of states and actions respectively, such that for $s, s' \in \mathcal{S}$ and $a \in \mathcal{A}$: $P(s'|a, s)$ is the probability that the system/agent transitions from s to s' given action a and $R(s', a, s)$ is a reward obtained by an agent transitioning from s to s' via a . A policy $\pi_\theta : \mathcal{S} \rightarrow \mathcal{A}$ is a (possibly randomized) mapping (parameterized by $\theta \in \mathbb{R}^d$) from \mathcal{S} to \mathcal{A} .

In model free on-policy RL, the goal is to optimize parameters θ of π_θ such that an agent deploying policy π_θ in the environment given by a fixed MDP maximizes total (expected/discounted) reward over a rollout time-step horizon H . In this paper we consider MDPs with finite horizons. In most

practical applications the dynamics of the MDP are not known and are often accessed through a simulator. One of the most popular classes of policy optimization techniques is the family of policy gradient (PG) methods [46, 45], which use backpropagation to make the policy favor actions which lead to higher rewards. Exploration (in the action space) is conducted by using stochastic policies and sampling actions $a \sim \pi_\theta(a|s)$.

Recent advances in Evolution Strategies (ES) methods for optimizing blackbox functions [42, 51, 3, 28] have shown that they can scale to high-dimensional RL settings. ES methods define the blackbox function $F : \mathbb{R}^d \rightarrow \mathbb{R}$ as taking as input parameters $\theta \in \mathbb{R}^d$ of a policy π_θ and outputting total discounted/expected reward obtained by an agent applying this policy in a given environment. As well as being trivially parallelizable, ES methods have been shown to produce more robust policies than their PG counterparts [23].

Since ES and PG both have differing strengths and weaknesses, there has been increasing cross-pollination with gradient-based techniques to learning, with hybrid approaches becoming popular [18, 17, 35, 10, 34]. Essentially, the key difference between ES and PG is the difference between exploring the environment via parameter or action space noise. While both have their own merits, they do not guarantee diverse behaviors will be considered by the policies.

Several recent methods in the neuroevolution community have made use of behavioral representations [4, 11]. A recent paper [4] proposed the use of a population of agents, each of which would seek to jointly maximize the reward and difference/*novelty* in comparison to other policies, quantified as the mean pairwise distance to other policies in the embedding space. Another approach, Evolvability ES [11] seeks to learn policies which can quickly adapt to a new task, by maximizing the variance or entropy of behaviors generated by a small perturbation. The MAP-Elites [30] algorithm is conceptually similar to ours, the authors seek to find quality solutions in differing dimensions. However, these dimensions need to be pre-specified, whereas our method can be considered a learned version of this approach. To the best of our knowledge, only one recent neuroevolutionary approach [15] uses the actions of a policy to represent behaviors, albeit in a genetic context over discrete actions.

There has recently been interest in unsupervised learning of diverse behaviors [8, 13]. These methods are similar in principle to novelty search without a reward signal, but instead focus on diversity in behaviors defined by the states they visit. Another class of algorithms making use of behavioral representations [12] focus on meta learning in the behavioral space, however they require pre-training on similar tasks in order to learn a new task. Another meta learning approach [41] proposes using a latent generative representation of model parameters, which could be thought of as a behavioral embedding of the policy. Finally, [54] propose a functional approach for learning diversified parameters. As an iterative method, this approach is still subject to the cycling phenomenon.

4 Neuroevolution for RL

Here we formalize existing methods for promoting diversity in population-based reinforcement learning.

4.1 Evolution Strategies

ES methods cast RL as a blackbox optimization problem. Since a blackbox function $F : \mathbb{R}^d \rightarrow \mathbb{R}$ may not even be differentiable, in practice its smoothed variants are considered. One of the most popular ones, the Gaussian smoothing [31] F_σ of a function F is defined as:

$$\begin{aligned} F_\sigma(\theta) &= \mathbb{E}_{\mathbf{g} \sim \mathcal{N}(0, \mathbf{I}_d)} [F(\theta + \sigma \mathbf{g})] \\ &= (2\pi)^{-\frac{d}{2}} \int_{\mathbb{R}^d} F(\theta + \sigma \mathbf{g}) e^{-\frac{\|\mathbf{g}\|^2}{2}} d\mathbf{g}, \end{aligned}$$

where $\sigma > 0$ is a hyperparameter quantifying the smoothing level. Even if F is nondifferentiable, we can easily obtain stochastic gradients for F_σ . The gradient of the Gaussian smoothing of F is given by the formula:

$$\nabla F_\sigma(\theta) = \frac{1}{\sigma} \mathbb{E}_{\mathbf{g} \sim \mathcal{N}(0, \mathbf{I}_d)} [F(\theta + \sigma \mathbf{g}) \mathbf{g}]. \quad (1)$$

This equation leads to several Monte Carlo gradient estimators used successfully in Evolution Strategies (ES, [42, 3]) algorithms for blackbox optimization in RL. Consequently, it provides gradient-based policy update rules such as:

$$\theta_{t+1} = \theta_t + \eta \frac{1}{k\sigma} \sum_{i=1}^k R_i \mathbf{g}_i, \quad (2)$$

where $R_i = F(\theta_t + \sigma \mathbf{g}_i)$ is the reward for perturbed policy $\theta_t + \sigma \mathbf{g}_i$ and $\eta > 0$ stands for the step size.

4.2 Novelty Search

In the context of population-based Reinforcement Learning, one prominent approach is the class of novelty search methods for RL [24, 25, 4]. The NSR-ES algorithm [4] maintains a meta-population of M agents, and at each iteration t sequentially samples and an individual member θ_t^m . This agent is perturbed with samples $\mathbf{g}_1^m, \dots, \mathbf{g}_k^m \sim \mathcal{N}(0, \mathbf{I}_d)$, and then the rewards $R_i^m = F(\theta_t^m + \sigma \mathbf{g}_i^m)$ and embeddings $\Phi(\theta_t^m + \sigma \mathbf{g}_i^m)$ are computed in parallel. The *novelty* of a given policy is then computed as the mean Euclidean distance of the policy embedding with the remaining members of the population $\Phi(\theta_i^m)$ for $i \neq m$. In order to update the policy, the rewards and novelty scores are normalized (denoted \hat{R}_i^m and \hat{N}_i^m), and the policy is updated as follows:

$$\theta_{t+1}^m = \theta_t^m + \frac{\eta}{k\sigma} \sum_{i=1}^k [(1 - \lambda) \hat{R}_i^m + \lambda \hat{N}_i^m] \mathbf{g}_i, \quad (3)$$

where novelty weight $\lambda > 0$ is a hyperparameter. Value $\lambda = 0$ corresponds to standard ES approach (see: Eq.2) whereas algorithm with $\lambda = 1$ neglects reward-signal and optimizes solely for diversity. A simple template of this approach, with a fixed population size, appears in Alg. 1.

Despite encouraging results on hard exploration environments, these algorithms contain several flaws. They lack a rigorous means to evaluate the diversity of the population as a whole, this means that M policies may fall into $N < M$ conjugacy classes, leading to the illusion of a diverse population on a mean pairwise Euclidean distance metric.

Algorithm 1 Population-Based NSR-ES

Input: : learning rate η , noise standard deviation σ , number of policies to maintain M , number of iterations T , embedding Φ , novelty weight λ .

Initialize: $\{\theta_0^1, \dots, \theta_0^M\}$.

for $t = 0, 1, \dots, T - 1$ **do**

1. Sample policy to update: $\theta_t^m \sim \{\theta_t^1, \dots, \theta_t^M\}$.
 2. Compute rewards $F(\theta_t^m + \sigma \mathbf{g}_k)$ for all $\mathbf{g}_1, \dots, \mathbf{g}_k$, sampled independently from $\mathcal{N}(0, \mathbf{I}_d)$.
 3. Compute embeddings $\Phi(\theta_t^m + \sigma \mathbf{g}_k)$ for all k .
 4. Let R_k and N_k be the normalized reward and novelty for each perturbation \mathbf{g}_k .
 5. Update Agent via Equation 3.
-

Ideally, we would guide optimization in a way which would evenly distribute policies in areas of the embedding space, which correspond to high rewards. The policy embeddings (BCs) used are based on heuristics which may not generalize to new environments [19]. The single sequential updates may lead high performing policies away from an improved reward (as is the case in the Humanoid experiment in [4]). Finally, cycles may become present, whereby the population moves from one area of the feature space to a new area and back again [30].

In the next section we address these issues, leveraging insights from Determinantal Point Processes (DPPs, [21]), and introduce the DvD algorithm.

5 Diversity via Determinants

In this section we present the key components of our algorithm, Diversity via Determinants (DvD). This entails introducing a new behavioral embedding, a means to jointly update the population via Determinants, and our adaptive exploration mechanism.

5.1 Task Agnostic Behavioral Embeddings

Many state of the art policy gradient algorithms [45, 46] consider a setting whereby a new policy $\pi_{\theta_{t+1}}$ is optimized with a constraint on the size of the update. The constraint is typically of the

following form:

$$\mathbb{E}_{s \sim \pi_{\theta_t}} [\mathbf{KL}[\pi_{\theta_t}(\cdot|s), \pi_{\theta_{t+1}}(\cdot|s)]] \leq \delta \quad (4)$$

for $\delta \geq 0$ and where \mathbf{KL} stands for KL-divergence. This requirement can be considered as a constraint on the behavior of the new policy [33]. Despite the remarkable success of these algorithms, there has been little consideration for action-based behavior embeddings in the neuroevolution community.

Inspired by this approach, we choose to represent policies with the actions they produce for given states. This idea is underpinned by the observations that if the number of states is finite then deterministic policies can be represented in tabular form. Thus trivially in this setting we have:

$$\Phi(\theta_1) = \Phi(\theta_2) \iff \pi_{\theta_1} = \pi_{\theta_2}, \quad (5)$$

where θ_1, θ_2 are vectorized parameters and the behavior embedding Φ is the concatenations of actions $a_i = \pi_{\theta}(a_i|s_i)$ for all $s_i \in S$. This approach allows us to represent the behavior of policies in vectorized form, as $\Phi : \theta \rightarrow \mathbb{R}^l$ where $l = m * n$, where m is the dimensionality of each action and n is the number of states.

Of course, in most practical settings the state space is intractably or infinitely large. Therefore, we must select the states $\{s_1, \dots, s_n\}$ to best represent the environment. In our experiments we used random sampling from the buffer, which corresponds to frequency weights. Other possibilities include selecting diverse ensembles of states via DPP-driven sampling or learning probabilistic functions which allow us to select states where we are most uncertain. We explore each of these choices in the experiments where we show the representative power of this action-based embedding is not overly sensitive to these design choices (see: Fig. 6).

5.2 Joint Population Update

Equipped with a novel approach for behavioral embeddings, we are now ready to present our mechanism for evaluating population-wide diversity. We first need to define a Determinantal Point Process (DPP, [21]):

Definition 5.1. (Determinantal Point Processes) Consider a finite set of datapoints $\mathcal{X} = \{\mathbf{x}^1, \dots, \mathbf{x}^N\}$, with $\mathbf{x}^i \in \mathbb{R}^d$. A determinantal point process is a distribution \mathcal{P} over the subsets of \mathcal{X} such that for some real, symmetric matrix \mathbf{K} indexed by the elements of \mathcal{X} the following holds for every subset $A \subseteq \mathcal{X}$:

$$\mathbb{P}(A \subseteq \mathcal{S}) = \det(\mathbf{K}_A), \quad (6)$$

where \mathcal{S} is sampled from \mathcal{P} and \mathbf{K}_A stands for the submatrix of \mathbf{K} obtained by taking rows and columns indexed by the elements of A . Matrix \mathbf{K} is positive semidefinite since all principal minors $\det(\mathbf{K}_A)$ are nonnegative.

In our setting we do not explicitly sample from a DPP, but leverage the mechanism to define population diversity as follows:

$$\text{Div}_t(\theta_t^1, \dots, \theta_t^M) = \det(K(\Phi(\theta_t^i), \Phi(\theta_t^j))_{i,j=1}^M), \quad (7)$$

where $K : \mathbb{R}^l \times \mathbb{R}^l \rightarrow \mathbb{R}$ is a given kernel function.

At every iteration we sample Mk Gaussian perturbation vectors $\{\mathbf{g}_i^m\}_{i=1, \dots, k}^{m=1, \dots, M}$. We use two partitionings of this Mk -element subset that illustrate our dual objective - high local rewards and large global diversity. The first partitioning assigns to i^{th} worker a set $\{\mathbf{g}_1^m, \dots, \mathbf{g}_k^m\}$. These are the perturbations used by the worker to compute its local rewards. The second partitioning splits $\{\mathbf{g}_i^m\}_{i=1, \dots, k}^{m=1, \dots, M}$ into subsets: $\mathcal{D}_i = \{\mathbf{g}_1^1, \dots, \mathbf{g}_i^M\}$. Instead of measuring the contribution of an individual \mathbf{g}_i^m to the diversity, we measure the contribution of the entire \mathcal{D}_i . This motivates the following definition:

$$\text{Div}_t(i) = \text{Div}_t(\theta_t^1 + \mathbf{g}_i^1, \dots, \theta_t^M + \mathbf{g}_i^M). \quad (8)$$

The update from Eq. 3 is then replaced by the following one:

$$\theta_{t+1}^m = \theta_t^m + \frac{\eta}{k\sigma} \sum_{i=1}^k [(1 - \lambda)R_i^m + \lambda \text{Div}_t(i)] \mathbf{g}_i^m. \quad (9)$$

Now that we have a method to jointly optimize a population with respect to its future diversity and local rewards, we turn our attention to the issue of choosing hyperparameter λ .

5.3 Adaptive Exploration

In the previous section we introduced a principled mechanism to jointly optimize the population for individual rewards and population-wide diversity. This addresses several of the key issues with existing novelty search methods, however, it still relies on a user-specified degree of priority for each of the two objectives (λ). We formalize this problem through the lens of multi-armed bandits, and introduce a means to adaptively select λ such that we encourage favoring the reward or diversity at different stages of optimization, using Thompson Sampling [53, 48, 1, 39, 40].

Let $\mathcal{K} = \{1, \dots, K\}$ denote a set of arms available to the decision maker (learner) who is interested in maximizing its expected cumulative reward. The optimal strategy for the learner is to pull the arm with the largest mean reward. Thompson Sampling is a mechanism whereby the learner maintains a mean reward model for each of the arms. At the beginning of each round the learner produces a sample mean from its mean reward model for each arm, and pulls the arm from which it obtained the largest sample. After observing the selected arm's reward it updates its mean reward model.

Let π_t^i be the learner's reward model for arm i at time t . When $t = 0$ the learner initializes each of its mean reward models to prior distributions $\{\pi_0^i\}_{i=1}^K$. At any other time $t > 0$, the learner starts by sampling mean reward candidates $\mu_i \sim \pi_{t-1}^i$ and pulling the arm:

$$i_t = \arg \max_{i \in \mathcal{K}} \mu_i. \quad (10)$$

After observing a true reward sample r_t from arm i_t , the learner updates its posterior distribution for arm i_t . All the posterior distributions over arms $i \neq i_t$ remain unchanged.

In this paper we make use of a Bernoulli model for the reward signal corresponding to the two arms ($\lambda = 0, \lambda = 0.5$). At any time t , the chosen arm's sample reward is the indicator variable $r_t = \mathbf{1}(R_{t+1} > R_t)$ where R_t denotes the reward observed at θ_t and R_{t+1} that at θ_{t+1} computed as in Equation 9. We make a simplifying stationarity assumption and disregard the changing nature of the arms' means in the course of optimization. The Bernoulli assumption makes the posterior updates quite simple. We use beta distributions to model both the priors and the posteriors of the arms' means. We add a more detailed description of the specifics of our methodology in the Appendix (see: Section 9).

We believe this adaptive mechanism could also be used for count-based exploration methods or intrinsic rewards [44], and note very recent work using a similar approach to vary exploration in off-policy methods [43].

5.4 DvD Algorithm

Combining these insights, we obtain the DvD algorithm presented in Algorithm 2. At each timestep, the set of policies $\Theta_t = \{\theta_t^1, \dots, \theta_t^M\}$ are simultaneously perturbed, with rewards computed locally and diversity computed globally. These two objectives are combined based on a dynamically changing λ value to produce a new population.

Algorithm 2 Diversity via Determinants (DvD)

Input: : learning rate η , noise standard deviation σ , number of policies to maintain M , number of perturbations k , number of iterations T , behavioral embedding Φ

Initialize: Policies $\Theta_0 = \{\theta_0^1, \dots, \theta_0^M\}$, $\lambda \sim [0, 0.5]$.

for $t = 0, 1, \dots, T - 1$ **do**

1. **Generate Samples:** Sample $\mathbf{g}_i^m \stackrel{\text{iid}}{\sim} \mathcal{N}(0, \mathbf{I}_d)$ perturbations for $i \in \{1, \dots, k\}$, $m \in \{1, \dots, M\}$.
 2. **Evaluate Samples:** Compute rewards $\{R_i^1, \dots, R_i^M\}$ and embeddings $\{\Phi_i^1, \dots, \Phi_i^M\}$ corresponding to perturbations for $i \in \{1, \dots, k\}$, where: $\Phi_i^m = \Phi(\theta_t^m + \mathbf{g}_i^m)$.
 3. **Calculate diversity for perturbations:** Compute $\text{Div}_t(i) = \det(\mathbf{K})$ where $\mathbf{K}_{ab} = K(\Phi_i^a, \Phi_i^b)$.
 4. **Sample λ :** Equation 10.
 5. **Update population:** Equation 9.
 6. Append states to buffer, and update λ 's posterior.
-

6 Experiments

In this section we seek to answer the following questions:

1. Does DvD find diverse solutions?
2. Does DvD also succeed with fruitful reward function?
3. How sensitive is DvD to the behavioral embedding design?

In addition we wish to evaluate the impact of individual components of our approach to quantify their importance.

To answer these questions, we consider a variety of settings, from simple environments with deceptive rewards, to challenging multi-modal environments inspired by the meta-learning literature. In all settings we compare our method against a vanilla ES (referred to as ES) which updates each population member sequentially, as well as NSR-ES from [4]. All experiments made use of the ray [29] library for parallel computing, with experiments run on a 32-core machine.

For both DvD and NSR-ES, we use the actions from 20 randomly selected states as the behavioral embedding for **all** experiments. We parameterize our policies with two hidden layer neural networks, with tanh activations. We vary the size of the hidden layers depending on the task, but keep the same settings across all algorithms (more details are in the Appendix, Section 8.2). All x-axes are presented in terms of iterations. Comparisons are made fair by dividing the for two sequential algorithms (ES and NSR-ES) by the population size.

6.1 Exploration

We begin our experiments with a simple environment, whereby a two dimensional point agent is given a reward equal to the negative distance away from a goal. The agent is separated from its goal by the wall (see: Fig 2a)).

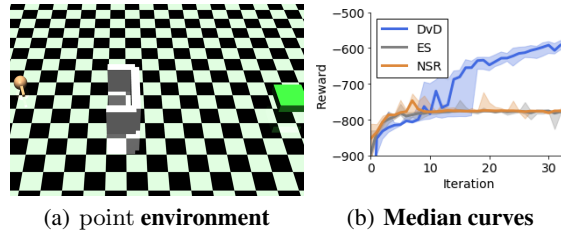


Figure 2: In this figure we show the median best performing agent across ten seeds on the task of reaching the goal while avoiding an obstacle.

We ran ten seeds for all three methods, with hyperparameters described in detail in the Appendix (Table 4). As we see, both vanilla ES and NSR-ES fail to get past the wall (a reward of -800), yet DvD is able to solve the environment for **all ten seeds**.

6.2 Finding Multiple Modes

A key attribute of a QD algorithm is the ability to learn a diverse set of high performing solutions. This is often demonstrated qualitatively, through videos of learned gaits, and thus hard to scientifically prove.

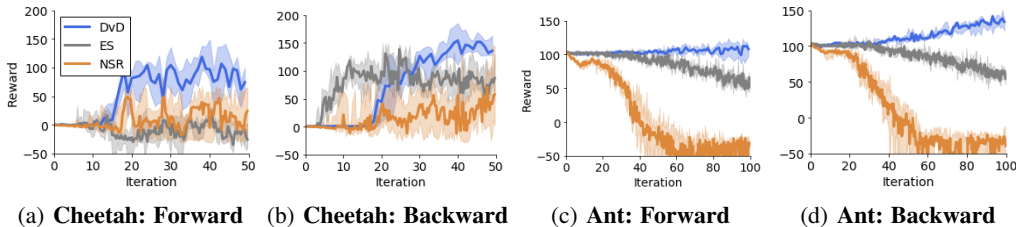
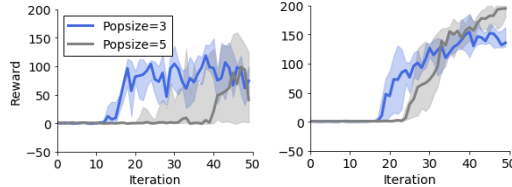


Figure 3: The median best performing agent across ten seeds for multi-mode tasks and two environments: Cheetah and Ant.

Here we have instead chosen to assess this quantitatively, by explicitly creating environments with multiple solutions. In these environments, the agent performs multiple tasks sequentially, and receives a reward at the end corresponding to the highest cumulative reward achieved in one individual task. It is then possible to evaluate the performance of each agent on the individual tasks, and thus explicitly test for high quality diverse behaviors.

Concretely, our environments are based on the Cheetah and Ant Forward and Backward tasks commonly used in meta-RL [9, 38]. In both settings we used a population size of $M = 3$. The results are presented in Fig. 3. We see that DvD is able to learn both modes in both environments, substantially outperforming ES and NSR-ES. For the Cheetah, the Backward task appears simpler to learn, and without the diversity term vanilla ES learns this task quickly, but subsequently performs poorly in the Forward task (which has an inverse reward function). For The Ant environment, it appears the noise from two separate tasks makes it impossible for vanilla ES to learn at all.

We also studied the relation between population size and the number of modes learned by the population. Both the tasks considered here have two modes, and intuitively a population of size $M = 3$ should be capable of learning both of them. However, we also considered the case for $M = 5$ (Fig. 4), and found that in fact a larger population was harmful for the performance. This leads to the interesting future work of adapting not only the degree of diversity but the size of the population.

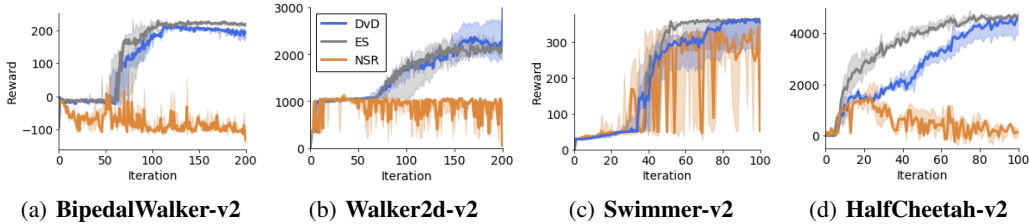


(a) **Cheetah: Forward** (b) **Cheetah: Backward**

Figure 4: Ablation study for the DvD algorithm: population size. The median best performing agent across ten seeds for the Cheetah multi-task environment. In all curves we have the same setting aside from population sizes of $M = 3$ and $M = 5$.

6.3 Single Mode Environments

In this section we consider the problem of optimizing tasks which may only contain one optimal solution (or at least, a smaller distance between optimal solutions in the behavioral space), and an informative reward function. In this case, overly promoting diversity may lead to worse performance on the task at hand, as seen in NSR-ES ([4], Fig. 1.(c)). We test this using four widely studied continuous control tasks from OpenAI Gym. In all cases we use a population size of $M = 5$, we provide additional experimental details in the Appendix (see Section 8.2).



(a) **BipedalWalker-v2** (b) **Walker2d-v2** (c) **Swimmer-v2** (d) **HalfCheetah-v2**

Figure 5: The median best performing agent across five seeds.

As we see in Fig. 5, in all four environments DvD shows a minimal drop in performance vs. the vanilla ES method which is solely focusing on the reward function. This promising result implies we gain the benefit of diversity without compromising on tasks where it is not required. We note that DvD outperforms in Walker2d, which is known to have a deceptive local optimum at 1000 induced by the survival bonus [28].

These experiments enable us also to demonstrate cyclic behaviour than standard novelty search approaches suffer from (see: Section 1). Interestingly, we often see NSR-ES initially performing well, demonstrating that the novelty is able to initially find good solutions. However, subsequent updates lead to degradation due to cycling.

6.4 Sensitivity of Performance to Behavioral Embedding Design

One of the crucial elements of this work is task-agnostic behavioral embedding. Similar to what has been used in all trust-region based policy gradient algorithms [45, 46], we use a concatenation of actions to represent policy behavior. In all experiments we used this behavioral embedding for both DvD and NSR, thus rendering the only difference between the two methods to be adaptive vs. fixed diversity and joint vs. individual updates.

However, there is still a question whether the design choices we made had an impact on performance. As such, we conducted a series of experiments to assess our choice of 20 randomly selected states for the behavioral embedding.

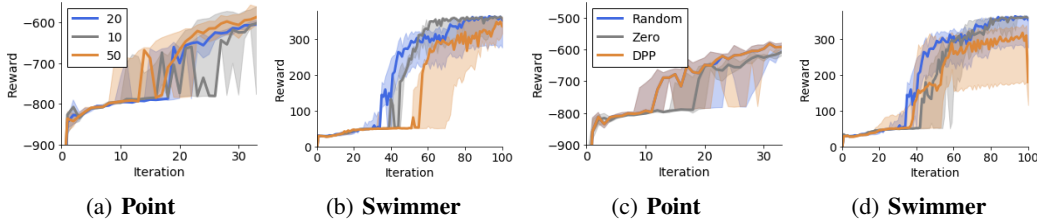


Figure 6: The median best performing agent across five seeds. In a) and b) we vary the number of states selected in the random sample, in c) and d) we select 20 states but using different mechanisms. Random corresponds to uniform sampling, Zero to a zero function trained on all seen states, where we select the maximum variance states. DPP stands for a k-DPP [20].

As we see in Fig. 6, both the number of states chosen and the mechanism for choosing them appear to have minimal impact on the performance. In all cases the point escapes the local maximum (of moving into the area surrounded by walls) and Swimmer reaches high rewards (> 300).

6.5 Results Discussion

We have shown that DvD can achieve the best of both worlds: exploratory benefits from promoting diversity when the reward function is deceptive or noisy, but crucially matching vanilla methods when it is not. This performance is down to both the joint update, which removes the cycling phenomenon, as well as the adaptive objective, which allows the algorithm to trade off diversity and reward during optimization.

In addition, we believe our behavioral embeddings can be used as the new standard for novelty search methods. We have shown these representations are robust to design choices, and can work across a variety of tasks without domain knowledge. This counteracts a key weakness of existing novelty search methods, as noted by [19]. We are excited by future work building upon this, potentially by learning embeddings.

In the Appendix (Section 8.1), we also test the importance of the adaptive mechanism, by comparing DvD vs. another variant with a fixed λ . In all cases, we see the adaptive method is outperforming its counterparts. Finally, we also show that DvD is invariant to the choice of the DPP kernel, with rigorous tests of six different popular kernels. Despite this, we believe exciting future work may be in a means to optimally select the kernel [7], or even learn one [55]. Intuitively, this could resemble learning the dimensions of behavior which we want to be diverse, an appealing thought, with connections to Hierarchical RL [22].

7 Conclusion and Future Work

In this paper we introduced a novel method (DvD) for promoting diversity in population-based methods for reinforcement learning. DvD addresses the issue of cycling in population-based methods by utilizing a joint population update, using ideas from Determinantal Point Processes. Furthermore, the adaptive mechanism facilitates flexible prioritization of diversity vs. reward, where the latter may often represent a strong signal for learning. We demonstrated across a variety of challenging tasks that our method not only finds diverse, high quality solutions but also manages to maintain strong performances in settings where there may only be one optimal solution.

We also note that DvD is not limited to ES-type algorithms. In fact, we also considered the policy gradient setting, and derived the gradient of the log determinant in Section 11 of the Appendix. That

might lead to new gradient-based diverse-population algorithms. We leave it and the comparison with related techniques [14, 6] to future work.

Acknowledgements

This work was conducted using resources provided by the GCP research credits program.

References

- [1] S. Agrawal and N. Goyal. Analysis of thompson sampling for the multi-armed bandit problem. In *Conference on Learning Theory*, pages 39–1, 2012.
- [2] K. Choromanski, A. Pacchiano, J. Parker-Holder, Y. Tang, D. Jain, Y. Yang, A. Iscen, J. Hsu, and V. Sindhwani. Provably robust blackbox optimization for reinforcement learning. In *The Conference on Robot Learning (CoRL)*, 2019.
- [3] K. Choromanski, M. Rowland, V. Sindhwani, R. E. Turner, and A. Weller. Structured evolution with compact architectures for scalable policy optimization. In *Proceedings of the 35th International Conference on Machine Learning, ICML 2018, Stockholmsmässan, Stockholm, Sweden, July 10-15, 2018*, pages 969–977, 2018.
- [4] E. Conti, V. Madhavan, F. P. Such, J. Lehman, K. O. Stanley, and J. Clune. Improving exploration in evolution strategies for deep reinforcement learning via a population of novelty-seeking agents. In *Proceedings of the 32Nd International Conference on Neural Information Processing Systems*, pages 5032–5043, USA, 2018. Curran Associates Inc.
- [5] A. Cully, J. Clune, D. Tarapore, and J.-B. Mouret. Robots that can adapt like animals. *Nature*, 521:503–507, 2015.
- [6] T. Doan, B. Mazouze, A. Durand, J. Pineau, and R. D. Hjelm. Attraction-repulsion actor-critic for continuous control reinforcement learning. *arXiv*, 2019.
- [7] D. Duvenaud, J. Lloyd, R. Grosse, J. Tenenbaum, and G. Zoubin. Structure discovery in nonparametric regression through compositional kernel search. In *Proceedings of the 30th International Conference on Machine Learning*, 2013.
- [8] B. Eysenbach, A. Gupta, J. Ibarz, and S. Levine. Diversity is all you need: Learning skills without a reward function. In *International Conference on Learning Representations*, 2019.
- [9] C. Finn, P. Abbeel, and S. Levine. Model-agnostic meta-learning for fast adaptation of deep networks. In *Proceedings of the 34th International Conference on Machine Learning*, volume 70 of *Proceedings of Machine Learning Research*, pages 1126–1135, 2017.
- [10] M. Fortunato, M. G. Azar, B. Piot, J. Menick, M. Hessel, I. Osband, A. Graves, V. Mnih, R. Munos, D. Hassabis, O. Pietquin, C. Blundell, and S. Legg. Noisy networks for exploration. In *International Conference on Learning Representations*, 2018.
- [11] A. Gajewski, J. Clune, K. O. Stanley, and J. Lehman. Evolvability es: Scalable and direct optimization of evolvability. In *Proceedings of the Genetic and Evolutionary Computation Conference, GECCO ’19*, pages 107–115, New York, NY, USA, 2019. ACM.
- [12] A. Gupta, R. Mendonca, Y. Liu, P. Abbeel, and S. Levine. Meta-reinforcement learning of structured exploration strategies. In S. Bengio, H. Wallach, H. Larochelle, K. Grauman, N. Cesa-Bianchi, and R. Garnett, editors, *Advances in Neural Information Processing Systems 31*, pages 5302–5311. Curran Associates, Inc., 2018.
- [13] K. Hartikainen, X. Geng, T. Haarnoja, and S. Levine. Dynamical distance learning for semi-supervised and unsupervised skill discovery. In *International Conference on Learning Representations*, 2020.
- [14] Z.-W. Hong, T.-Y. Shann, S.-Y. Su, Y.-H. Chang, T.-J. Fu, and C.-Y. Lee. Diversity-driven exploration strategy for deep reinforcement learning. In *Advances in Neural Information Processing Systems 31*. 2018.

- [15] E. C. Jackson and M. Daley. Novelty search for deep reinforcement learning policy network weights by action sequence edit metric distance. In *Proceedings of the Genetic and Evolutionary Computation Conference Companion*, GECCO 19, page 173174, New York, NY, USA, 2019. Association for Computing Machinery.
- [16] S. Khadka, S. Majumdar, S. Miret, S. McAleer, and K. Tumer. Evolutionary reinforcement learning for sample-efficient multiagent coordination, 2019.
- [17] S. Khadka, S. Majumdar, T. Nassar, Z. Dwiell, E. Tumer, S. Miret, Y. Liu, and K. Tumer. Collaborative evolutionary reinforcement learning. In K. Chaudhuri and R. Salakhutdinov, editors, *Proceedings of the 36th International Conference on Machine Learning*, volume 97 of *Proceedings of Machine Learning Research*, pages 3341–3350, Long Beach, California, USA, 09–15 Jun 2019. PMLR.
- [18] S. Khadka and K. Tumer. Evolution-guided policy gradient in reinforcement learning. In S. Bengio, H. Wallach, H. Larochelle, K. Grauman, N. Cesa-Bianchi, and R. Garnett, editors, *Advances in Neural Information Processing Systems 31*, pages 1188–1200. Curran Associates, Inc., 2018.
- [19] S. Kistemaker and S. Whiteson. Critical factors in the performance of novelty search. In *Proceedings of the 13th Annual Conference on Genetic and Evolutionary Computation*, GECCO 11, page 965972, New York, NY, USA, 2011. Association for Computing Machinery.
- [20] A. Kulesza and B. Taskar. k-dpps: Fixed-size determinantal point processes. In *Proceedings of the 28th International Conference on Machine Learning, ICML 2011, Bellevue, Washington, USA, June 28 - July 2, 2011*, pages 1193–1200, 2011.
- [21] A. Kulesza and B. Taskar. *Determinantal Point Processes for Machine Learning*. Now Publishers Inc., Hanover, MA, USA, 2012.
- [22] T. D. Kulkarni, K. Narasimhan, A. Saeedi, and J. Tenenbaum. Hierarchical deep reinforcement learning: Integrating temporal abstraction and intrinsic motivation. In D. D. Lee, M. Sugiyama, U. V. Luxburg, I. Guyon, and R. Garnett, editors, *Advances in Neural Information Processing Systems 29*, pages 3675–3683. Curran Associates, Inc., 2016.
- [23] J. Lehman, J. Chen, J. Clune, and K. O. Stanley. ES is more than just a traditional finite difference approximator. *arXiv preprint:1712.06568*, 2017.
- [24] J. Lehman and K. O. Stanley. Exploiting open-endedness to solve problems through the search for novelty. In *Proceedings of the Eleventh International Conference on Artificial Life (Alife XI)*. MIT Press, 2008.
- [25] J. Lehman and K. O. Stanley. Abandoning objectives: Evolution through the search for novelty alone. *Evolutionary Computation*, 19(2):189–223, 2011.
- [26] A. Li, O. Spyra, S. Perel, V. Dalibard, M. Jaderberg, C. Gu, D. Budden, T. Harley, and P. Gupta. A generalized framework for population based training. *CoRR*, abs/1902.01894, 2019.
- [27] S. Liu, G. Lever, N. Heess, J. Merel, S. Tunyasuvunakool, and T. Graepel. Emergent coordination through competition. In *International Conference on Learning Representations*, 2019.
- [28] H. Mania, A. Guy, and B. Recht. Simple random search provides a competitive approach to reinforcement learning. *CoRR*, abs/1803.07055, 2018.
- [29] P. Moritz, R. Nishihara, S. Wang, A. Tumanov, R. Liaw, E. Liang, W. Paul, M. I. Jordan, and I. Stoica. Ray: A distributed framework for emerging AI applications. *CoRR*, abs/1712.05889, 2017.
- [30] J.-B. Mouret and J. Clune. Illuminating search spaces by mapping elites. *ArXiv*, abs/1504.04909, 2015.
- [31] Y. Nesterov and V. Spokoiny. Random gradient-free minimization of convex functions. *Found. Comput. Math.*, 17(2):527–566, Apr. 2017.

- [32] I. Osband, C. Blundell, A. Pritzel, and B. Van Roy. Deep exploration via bootstrapped dqn. In D. D. Lee, M. Sugiyama, U. V. Luxburg, I. Guyon, and R. Garnett, editors, *Advances in Neural Information Processing Systems 29*, pages 4026–4034. Curran Associates, Inc., 2016.
- [33] A. Pacchiano, J. Parker-Holder, Y. Tang, A. Choromanska, K. Choromanski, and M. I. Jordan. Behavior guided reinforcement learning. *arXiv*, 2019.
- [34] M. Plappert, R. Houthooft, P. Dhariwal, S. Sidor, R. Y. Chen, X. Chen, T. Asfour, P. Abbeel, and M. Andrychowicz. Parameter space noise for exploration. In *International Conference on Learning Representations*, 2018.
- [35] Pourchot and Sigaud. CEM-RL: Combining evolutionary and gradient-based methods for policy search. In *International Conference on Learning Representations*, 2019.
- [36] J. K. Pugh, L. B. Soros, and K. O. Stanley. Quality diversity: A new frontier for evolutionary computation. *Frontiers in Robotics and AI*, 3:40, 2016.
- [37] B. Recht, C. Re, S. Wright, and F. Niu. Hogwild: A lock-free approach to parallelizing stochastic gradient descent. In *Advances in neural information processing systems*, pages 693–701, 2011.
- [38] J. Rothfuss, D. Lee, I. Clavera, T. Asfour, and P. Abbeel. ProMP: Proximal meta-policy search. In *International Conference on Learning Representations*, 2019.
- [39] D. Russo, B. Roy, A. Kazerouni, and I. Osband. A tutorial on thompson sampling. *Foundations and Trends in Machine Learning*, 11, 07 2017.
- [40] D. Russo and B. Van Roy. An information-theoretic analysis of thompson sampling. *J. Mach. Learn. Res.*, 17(1):24422471, Jan. 2016.
- [41] A. A. Rusu, D. Rao, J. Sygnowski, O. Vinyals, R. Pascanu, S. Osindero, and R. Hadsell. Meta-learning with latent embedding optimization. In *International Conference on Learning Representations*, 2019.
- [42] T. Salimans, J. Ho, X. Chen, S. Sidor, and I. Sutskever. Evolution strategies as a scalable alternative to reinforcement learning. *arXiv*, abs/1703.03864, 2017.
- [43] T. Schaul, D. Borsa, D. Ding, D. Szepesvari, G. Ostrovski, W. Dabney, and S. Osindero. Adapting behaviour for learning progress, 2019.
- [44] J. Schmidhuber. Formal theory of creativity, fun, and intrinsic motivation (19902010). *IEEE Transactions on Autonomous Mental Development*, 2(3):230–247, Sep. 2010.
- [45] J. Schulman, S. Levine, P. Abbeel, M. Jordan, and P. Moritz. Trust region policy optimization. In *International Conference on Machine Learning (ICML)*, 2015.
- [46] J. Schulman, F. Wolski, P. Dhariwal, A. Radford, and O. Klimov. Proximal policy optimization algorithms. *arXiv preprint arXiv:1707.06347*, 2016-2018.
- [47] A. Slivkins. Introduction to multi-armed bandits. *Foundations and Trends in Machine Learning*, 12(1-2):1–286, 2019.
- [48] N. Srinivas, A. Krause, S. Kakade, and M. Seeger. Gaussian process optimization in the bandit setting: No regret and experimental design. In *Proceedings of the 27th International Conference on International Conference on Machine Learning*, ICML10, page 10151022, Madison, WI, USA, 2010. Omnipress.
- [49] K. Stanley, J. Clune, J. Lehman, and R. Miikkulainen. Designing neural networks through neuroevolution. *Nature Machine Intelligence*, 1, 01 2019.
- [50] R. P. Stanley. Enumerative combinatorics volume 1 second edition. *Cambridge studies in advanced mathematics*, 2011.
- [51] F. P. Such, V. Madhavan, E. Conti, J. Lehman, K. O. Stanley, and J. Clune. Deep neuroevolution: Genetic algorithms are a competitive alternative for training deep neural networks for reinforcement learning. *CoRR*, abs/1712.06567, 2017.

- [52] R. S. Sutton and A. G. Barto. *Introduction to Reinforcement Learning*. MIT Press, Cambridge, MA, USA, 1st edition, 1998.
- [53] W. R. Thompson. On the likelihood that one unknown probability exceeds another in view of the evidence of two samples. *Biometrika*, 25(3/4):285–294, 1933.
- [54] D. Wang and Q. Liu. Nonlinear stein variational gradient descent for learning diversified mixture models. In K. Chaudhuri and R. Salakhutdinov, editors, *Proceedings of the 36th International Conference on Machine Learning*, volume 97 of *Proceedings of Machine Learning Research*, pages 6576–6585, Long Beach, California, USA, 09–15 Jun 2019. PMLR.
- [55] A. G. Wilson, Z. Hu, R. Salakhutdinov, and E. P. Xing. Deep kernel learning. In *Proceedings of the 19th International Conference on Artificial Intelligence and Statistics*, volume 51 of *Proceedings of Machine Learning Research*, pages 370–378, Cadiz, Spain, 2016.

Appendix

8 Additional Experiment Details

8.1 Ablation Studies

Here we seek to analyze the sensitivity of DvD to design choices made, in order to gain confidence surrounding the robustness of our method.

Do we need to adapt? In Fig 7 we evaluate the effectiveness of the adaptive mechanism, by running five experiments with the DvD algorithm with fixed λ . While notably we still see strong performance from the joint diversity score (vs. NSR ES in Fig 5), it is clear the adaptive mechanism boosts performance in all cases.

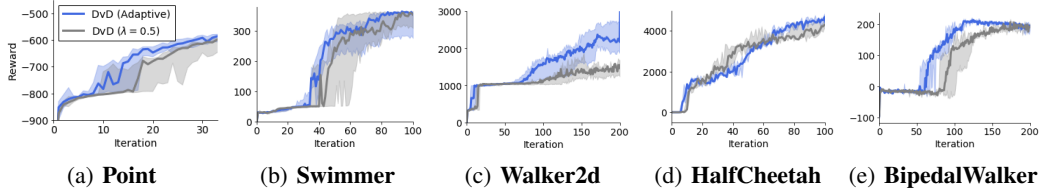


Figure 7: In this figure we show the median maximum performing agent across five seeds. The only difference between the two curves is the adaptive selection of λ .

Choice of DPP kernel For this work, we used the Squared Exponential (or RBF) kernel for all experiments. This decision was made due to its widespread use in the machine learning community and many desirable properties. However, in order to assess the quality of our method it is important to consider the sensitivity to the choice of kernel.

In Fig 8 and Table 8.1 we show the result from 5 seeds for a variety of kernels. As we see, in almost all cases the performance is strong, and similar to the Squared Exponential used in the main experiments.

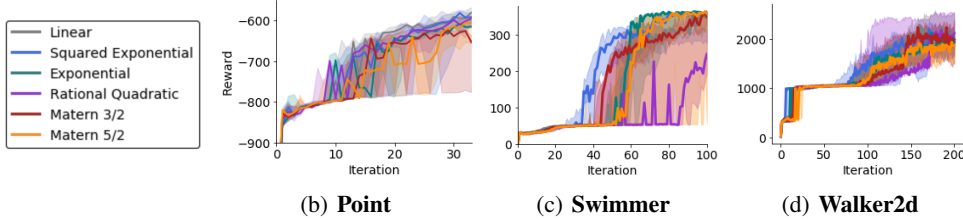


Figure 8: In this figure we show the median maximum performing agent across five seeds. The only difference between the two curves is the choice of kernel for the behavioral similarity matrix.

Table 1: This table shows the median maximum performing agent across 5 seeds. All algorithms shown are identical aside from the choice of DPP kernel. For point results are the best at 50 iterations, while for point it is 100 and Walker2d it is 200.

	Point	Swimmer	Walker2d
Squared Exponential	-547.03	354.86	1925.86
Exponential	-561.13	362.83	1929.81
Linear	-551.48	354.37	1944.95
Rational Quadratic	-548.55	246.68	2113.02
Matern $\frac{3}{2}$	-578.05	349.52	1981.66
Matern $\frac{5}{2}$	-557.69	357.88	1866.56

8.2 Hyperparameters

In Table 2 we show the method for generating behavioral embeddings used for NSR-ES and our method. We used these settings across **all** experiments, and did not tune them. Number of states corresponds to the number of states used for the embedding, which is the concatenation of the actions from a policy on those states. State selection refers to the mechanism for selecting the states from the buffer of all states seen on the previous iteration. The update frequency is how frequently we re-sample states to use for the embeddings. We do not want this to be too frequent or we will have different embeddings every iteration simply as a result of the changing states.

Table 2: Configuration for the behavioral embedding, used across all experiments for our method and NSR-ES.

	Value
Number of states	20
State selection	random
Update frequency	20

In Table 3 we show the hyperparameters used for the multi-modal experiments. We note the main difference between the two environments is the Ant requires more ES sensings (300 vs. 100) and a larger neural network (64-64 vs. 32-32) than the Cheetah. These settings were used for all three algorithms studied.

Table 3: Parameter configurations for the multi-modal experiments.

	Cheetah	Ant
σ	0.001	0.001
η	0.001	0.001
h	32	64
ES-sensings	100	300
State Filter	True	True

In Table 4 we show the hyperparameters used for the uni-model and deceptive reward experiments. The main difference is the size of the neural network for point and Swimmer is smaller (16-16 vs. 32-32) since these environments have smaller state and action dimensions than the others. In addition, we note the horizon H for the point is smaller, as 50 timesteps is sufficient to reach the goal. These settings were used for all three algorithms considered.

Table 4: Parameter configurations for the single mode experiments. The only difference across all tasks was a smaller neural network used for Swimmer and point, since they have a smaller state and action dimensionality.

	point	Swimmer	HalfCheetah	Walker2d	BipedalWalker
σ	0.1	0.1	0.1	0.1	0.1
η	0.05	0.05	0.05	0.05	0.05
h	16	16	32	32	32
ES-sensings	100	100	100	100	100
State Filter	True	True	True	True	True
H	50	1000	1000	1000	1600

9 Thomson Sampling

Let’s start by defining the Thomson Sampling updates for Bernoulli random variables. We borrow the notation from Section 5.3. Let $\mathcal{K} = \{1, \dots, K\}$ be a set of Bernoulli arms with mean parameters $\{\mu_i\}_{i=1}^K$.

Denote by π_t^i the learner’s mean reward model for arm i at time t . We let the learner begin with an independent prior belief over each μ_i , which we denote π_o^i . These priors are beta-distributed with parameters $\alpha_i^o = 1, \beta_i^o = 1$:

$$\pi_o^i(\mu) = \frac{\Gamma(\alpha_i^o + \beta_i)}{\Gamma(\alpha_i^o)\Gamma(\beta_i)} \mu^{\alpha_i^o-1} (1-\mu)^{\beta_i-1},$$

Where Γ denotes the gamma function. It is convenient to use beta distributions because of their conjugacy properties. It can be shown that whenever we use a beta prior, the posterior distribution is also a beta distribution. Denote α_i^t, β_i^t as the values of parameters α_i, β_i at time t .

Let i_t be the arm selected by Thomson Sampling as in Equation 10 at time t . After observing reward $r_t \in \{0, 1\}$ the arms posteriors are updated as follows:

$$(\alpha_i^{t+1}, \beta_i^{t+1}) = \begin{cases} (\alpha_i^t + r_t, \beta_i^t + (1 - r_t)) & \text{if } i = i_t \\ (\alpha_i^t, \beta_i^t) & \text{o.w.} \end{cases}$$

10 Determinants vs. Distances

In this section we consider the following question. Let $k(\mathbf{x}, \mathbf{y}) = \exp(-\|x - y\|^2)$. And $\mathbf{K} \in \mathbb{R}^{M \times M}$ be the kernel matrix corresponding to M agents and resulting of computing the Kernel dot products between their corresponding embeddings $\{\mathbf{x}_1, \dots, \mathbf{x}_M\}$:

Theorem 10.1. *For $M \leq 3$, the first order approximation of $\det(\mathbf{K})$ is proportional to the sum of the pairwise distances between $\{\mathbf{x}_1, \dots, \mathbf{x}_M\}$. For $M > 3$ this first order approximation equals 0.*

Proof. Consider the case of a population size $M = 3$, some policy embedding ϕ_i and the exponentiated quadratic kernel. In this setting, the diversity, measured by the determinant of the kernel (or similarity) matrix is as follows:

$$\begin{aligned} \det(\mathbf{K}) &= \begin{vmatrix} 1 & k(\mathbf{x}_1, \mathbf{x}_2) & k(\mathbf{x}_1, \mathbf{x}_3) \\ k(\mathbf{x}_2, \mathbf{x}_1) & 1 & k(\mathbf{x}_2, \mathbf{x}_3) \\ k(\mathbf{x}_3, \mathbf{x}_1) & k(\mathbf{x}_3, \mathbf{x}_2) & 1 \end{vmatrix} \\ &= 1 - k(\mathbf{x}_2, \mathbf{x}_3)k(\mathbf{x}_3, \mathbf{x}_2) - k(\mathbf{x}_1, \mathbf{x}_2)(k(\mathbf{x}_2, \mathbf{x}_1) - k(\mathbf{x}_3, \mathbf{x}_1)k(\mathbf{x}_2, \mathbf{x}_3)) \\ &\quad + k(\mathbf{x}_1, \mathbf{x}_3)(k(\mathbf{x}_2, \mathbf{x}_1)k(\mathbf{x}_3, \mathbf{x}_2) - k(\mathbf{x}_3, \mathbf{x}_1)) \\ &= 1 - k(\mathbf{x}_1, \mathbf{x}_2)^2 - k(\mathbf{x}_1, \mathbf{x}_3)^2 - k(\mathbf{x}_2, \mathbf{x}_3)^2 + 2k(\mathbf{x}_1, \mathbf{x}_2)k(\mathbf{x}_1, \mathbf{x}_3)k(\mathbf{x}_2, \mathbf{x}_3) \end{aligned}$$

So if we take k to be the squared exponential kernel:

$$\begin{aligned} &= 1 - \exp\left(\frac{-\|x_1 - x_2\|^2}{l}\right) - \exp\left(\frac{-\|x_1 - x_3\|^2}{l}\right) - \exp\left(\frac{-\|x_2 - x_3\|^2}{l}\right) \\ &\quad + 2 \exp\left(\frac{-\|x_1 - x_2\|^2 - \|x_1 - x_3\|^2 - \|x_2 - x_3\|^2}{2l}\right) \end{aligned}$$

Recall that for $|x| \ll 1$ small enough, $\exp(x) \approx 1 + x$. Substituting this approximation in the expression above we see:

$$\begin{aligned} \det(\mathbf{K}) &\approx \|x_1 - x_2\|^2 + \|x_1 - x_3\|^2 + \|x_2 - x_3\|^2 - \frac{\|x_1 - x_2\|^2 + \|x_1 - x_3\|^2 + \|x_2 - x_3\|^2}{2} \\ &= \frac{\|x_1 - x_2\|^2 + \|x_1 - x_3\|^2 + \|x_2 - x_3\|^2}{2} \end{aligned}$$

Which is essentially the mean pairwise l_2 distance. What can we say about these differences (e.g. exp vs. not)? Does this same difference generalize to $M > 3$?

Approximation for $M > 3$

Recall that for a matrix $\mathbf{A} \in \mathbb{R}^{M \times M}$, the determinant can be written as:

$$\det(\mathbf{A}) = \sum_{\sigma \in \mathbb{S}_M} \text{sign}(\sigma) \prod_{i=1}^M \mathbf{A}_{i, \sigma(i)}$$

Where \mathbb{S}_M denotes the symmetric group over M elements. Lets identify $A_{i,j} = \exp\left(-\frac{\|x_i - x_j\|^2}{2}\right)$. Notice that for any $\sigma \in \mathbb{S}_M$, we have the following approximation:

$$\prod_{i=1}^M A_{i,\sigma(i)} \approx 1 - \sum_{i=1}^M \frac{\|x_i - x_{\sigma(i)}\|^2}{2} \quad (11)$$

Whenever for all $i, j \in [M]$ the value of $\|x_i - x_j\|^2$ is small.

We are interested in using this termwise approximation to compute an estimate of $\det(\mathbf{A})$. Plugging the approximation in Equation 11 into the formula for the determinant yields the following:

$$\begin{aligned} \det(\mathbf{A}) &\approx \sum_{\sigma \in \mathbb{S}_M} \text{sign}(\sigma) \left(1 - \sum_{i=1}^M \frac{\|x_i - x_{\sigma(i)}\|^2}{2} \right) \\ &= \underbrace{\sum_{\sigma \in \mathbb{S}_M} \text{sign}(\sigma)}_I - \underbrace{\sum_{\sigma \in \mathbb{S}_M} \text{sign}(\sigma) \sum_{i=1}^M \frac{\|x_i - x_{\sigma(i)}\|^2}{2}}_{II} \end{aligned}$$

Term I equals zero as it is the sum of all signs of the permutations of \mathbb{S}_n and $n > 1$.

In order to compute the value of II we observe that by symmetry:

$$II = B \sum_{i < j} \|x_i - x_j\|^2$$

For some $B \in \mathbb{R}$. We show that $B = 0$ for $M > 3$. Let's consider the set $B_{1,2}$ of permutations $\sigma \in \mathbb{S}_M$ for which the sum $\sum_{i=1}^M \frac{\|x_i - x_{\sigma(i)}\|^2}{2}$ contains the term $\frac{\|x_1 - x_2\|^2}{2}$. Notice that $B = \frac{1}{2} \sum_{\sigma \in B_{1,2}} \text{sign}(\sigma)$. Let's characterize $B_{1,2}$ more exactly.

Recall every permutation $\sigma \in \mathbb{S}_M$ can be thought of as a product of cycles. For more background on the cycle decomposition of permutations see [50].

The term $\frac{\|x_1 - x_2\|^2}{2}$ appears whenever the cycle decomposition of σ contains a transition of the form $1 \rightarrow 2$ or $1 \leftarrow 2$. It appears twice if the cycle decomposition of σ has the cycle corresponding to a single transposition $1 \leftrightarrow 2$.

Let $\vec{B}_{1,2}$ be the set of permutations containing a transition of the form $1 \rightarrow 2$ (and no transition of the form $1 \leftarrow 2$) $\overleftarrow{B}_{1,2}$ be the set of permutations containing a transition of the form $1 \leftarrow 2$ (and no transition of the form $1 \rightarrow 2$) and finally $\overleftrightarrow{B}_{1,2}$ be the set of permutations containing the transition $1 \leftrightarrow 2$.

Notice that:

$$B = \underbrace{\sum_{\sigma \in \vec{B}_{1,2}} \text{sign}(\sigma)}_{O_1} + \underbrace{\sum_{\sigma \in \overleftarrow{B}_{1,2}} \text{sign}(\sigma)}_{O_2} + 2 \underbrace{\sum_{\sigma \in \overleftrightarrow{B}_{1,2}} \text{sign}(\sigma)}_{O_3}$$

We start by showing that for $M > 3$, $O_3 = 0$. Indeed, any $\sigma \in \overleftrightarrow{B}_{1,2}$ has the form $\sigma = (1, 2)\sigma'$ where σ' is the cycle decomposition of a permutation over $3, \dots, M$. Consequently $\text{sign}(\sigma) = -\text{sign}(\sigma')$. Iterating over all possible $\sigma' \in \mathbb{S}_{M-2}$ permutations over $[3, \dots, M]$ yields the set $\overleftrightarrow{B}_{1,2}$ and therefore:

$$\begin{aligned} O_3 &= - \sum_{\sigma' \in \mathbb{S}_{M-2}} \text{sign}(\sigma') \\ &= 0 \end{aligned}$$

The last equality holds because $M - 2 \geq 2$. We proceed to analyze the terms O_1 and O_2 . By symmetry it is enough to focus on O_1 . Let c be a fixed cycle structure containing the transition $1 \rightarrow 2$. Any $\sigma \in \vec{B}_{1,2}$ containing c can be written as $\sigma = c\sigma'$ where σ' is a permutation over the remaining elements of $\{1, \dots, M\} \setminus c$ and therefore $\text{sign}(\sigma) = (-1)^{|c|-1} \text{sign}(\sigma')$. Let $\vec{B}_{1,2}^c$ be the subset of $\vec{B}_{1,2}$ containing c .

Notice that:

$$O_1 = \sum_{c|1 \rightarrow 2 \in c, |c| \geq 3} \underbrace{\left[\sum_{\sigma \in \vec{B}_{1,2}^c} \text{sign}(\sigma) \right]}_{O_1^c}$$

Let's analyze O_1^c :

$$\begin{aligned} O_1^c &= \sum_{\sigma \in \vec{B}_{1,2}^c} \text{sign}(\sigma) \\ &= (-1)^{|c|-1} \sum_{\sigma \in \mathbb{S}_{M-|c|}} \text{sign}(\sigma) \end{aligned}$$

If $|\{1, \dots, M\} \setminus c| \geq 2$ this quantity equals zero. Otherwise it equals $(-1)^{|c|-1}$. We recognize two cases, when $|\{1, \dots, M\} \setminus c| = 0$ and when $|\{1, \dots, M\} \setminus c| = 1$. The following decomposition holds^{*}:

$$\begin{aligned} O_1 &= |\{c|1 \rightarrow 2 \in c, |c| \geq 3|\{1, \dots, M\} \setminus c| = 0\}| * (-1)^{M-1} \\ &\quad + |\{c|1 \rightarrow 2 \in c, |c| \geq 3|\{1, \dots, M\} \setminus c| = 1\}| * (-1)^{M-2} \end{aligned}$$

A simple combinatorial argument shows that:

$$|\{c|1 \rightarrow 2 \in c, |\{1, \dots, M\} \setminus c| = 0\}| = (M - 2)!$$

Roughly speaking this is because in order to build a size M cycle containing the transition $1 \rightarrow 2$, we only need to decide on the positions of the next $M - 2$ elements, which can be shuffled in $M - 2$ ways. Similarly, a simple combinatorial argument shows that:

$$|\{c|1 \rightarrow 2 \in c, |\{1, \dots, M\} \setminus c| = 1\}| = (M - 2)!$$

A similar counting argument yields this result. First, there are $M - 2$ ways of choosing the element that will not be in the cycle. Second, there are $(M - 3)!$ ways of arranging the remaining elements to fill up the $M - 3$ missing slots of the $M - 1$ sized cycle c .

We conclude that in this case $O_1 = 0$.

□

This result implies two things:

1. When $M \leq 3$. If the gradient of the embedding vectors is sufficiently small, the determinant penalty is up to first order terms equivalent to a pairwise distances score. This may not be true if the embedding vector's norm is large.
2. When $M > 3$. The determinant diversity penalty variability is given by its higher order terms. It is therefore not equivalent to a pairwise distances score.

^{*}Here we use the assumption $M \geq 4$ to ensure that both $|\{c|1 \rightarrow 2 \in c, |c| \geq 3|\{1, \dots, M\} \setminus c| = 0\}| > 0$ and $|\{c|1 \rightarrow 2 \in c, |c| \geq 3|\{1, \dots, M\} \setminus c| = 1\}| > 0$.

11 Policy Gradient Formulation

In the case of Deterministic behavioral embeddings, it is possible to compute gradients through the whole objective. Notice that $\det(\mathbf{K})$ is then differentiable as a function of the policy parameters. In the case of trajectory based embeddings, differentiating through the determinant is not that simple. Actually it may make sense in this case to use a $\log(\det(\mathbf{K}))$ score instead. This is because of the following lemmas:

Lemma 11.1. *The gradient of $\log(\det(\mathbf{K}))$ with respect to $\theta = \theta^1, \dots, \theta^M$ equals:*

$$\nabla_{\theta} \log(\det(\mathbf{K})) = -(\nabla_{\theta} \Phi(\theta)) (\nabla_{\Phi} \mathbf{K}) \mathbf{K}^{-1}$$

Where $\Phi(\theta) = \Phi(\theta^1) \dots \Phi(\theta^M)$

Proof. We start with:

$$\nabla_{\mathbf{K}} \log(\det(\mathbf{K})) = -\mathbf{K}^{-1}$$

This is a known result^{*}.

Consequently,

$$\begin{aligned} \nabla_{\theta} \log(\det(\mathbf{K})) &= (\nabla_{\theta} \Phi(\theta)) (\nabla_{\Phi} \mathbf{K}) (\nabla_{\mathbf{K}} \log(\det(\mathbf{K}))) \\ &= -(\nabla_{\theta} \Phi(\theta)) (\nabla_{\Phi} \mathbf{K}) \mathbf{K}^{-1} \end{aligned}$$

Each of the other gradients can be computed exactly.

□

^{*}see for example <https://math.stackexchange.com/questions/38701/how-to-calculate-the-gradient-of-log-det-matrix-inverse>